

PROBING THE METAL ENRICHMENT OF THE INTERGALACTIC MEDIUM AT $Z = 5 - 6$ USING THE HUBBLE SPACE TELESCOPE

ZHENG CAI^{1,8}, XIAOHUI FAN², ROMEEL DAVE^{3,4,5}, KRISTIAN FINLATOR⁶, BEN OPPENHEIMER⁷

¹ UCO/Lick Observatory, University of California, 1156 High Street, Santa Cruz, CA 95064, USA; zcai@ucolick.org

² Steward Observatory, University of Arizona, 933 North Cherry Avenue, Tucson, AZ, 85721, USA

³ Institute for Astronomy, University of Edinburgh, Royal Observatory, Edinburgh, EH9 3HJ

⁴ University of the Western Cape, Bellville, Cape Town 7535, South Africa

⁵ South African Astronomical Observatories, Observatory, Cape Town 7925, South Africa

⁶ New Mexico State University, Las Cruces, NM 88003, USA

⁷ CASA, Department of Astrophysical and Planetary Sciences, University of Colorado, 389 UCB, Boulder, CO 80309, USA and

⁸ Hubble Fellow

Accepted by The Astrophysical Journal Letter

ABSTRACT

We test the galactic outflow model by probing associated galaxies of four strong intergalactic CIV absorbers at $z = 5-6$ using the Hubble Space Telescope (HST) ACS ramp narrowband filters. The four strong CIV absorbers reside at $z = 5.74, 5.52, 4.95,$ and 4.87 , with column densities ranging from $N_{\text{CIV}} = 10^{13.8} \text{ cm}^{-2}$ to $10^{14.8} \text{ cm}^{-2}$. At $z = 5.74$, we detect an *i*-dropout Ly α emitter (LAE) candidate with a projected impact parameter of 42 physical kpc from the CIV absorber. This LAE candidate has a Ly α -based star formation rate ($\text{SFR}_{\text{Ly}\alpha}$) of $2 M_{\odot} \text{ yr}^{-1}$ and a UV-based SFR of $4 M_{\odot} \text{ yr}^{-1}$. Although we cannot completely rule out that this *i*-dropout emitter may be an [OII] interloper, its measured properties are consistent with the CIV powering galaxy at $z = 5.74$. For CIV absorbers at $z = 4.95$ and $z = 4.87$, although we detect two LAE candidates with impact parameters of 160 kpc and 200 kpc, such distances are larger than that predicted from the simulations. Therefore we treat them as non-detections. For the system at $z = 5.52$, we do not detect LAE candidates, placing a $3\text{-}\sigma$ upper limit of $\text{SFR}_{\text{Ly}\alpha} \approx 1.5 M_{\odot} \text{ yr}^{-1}$. In summary, in these four cases, we only detect one plausible CIV source at $z = 5.74$. Combining the modest SFR of the one detection and the three non-detections, our HST observations strongly support that smaller galaxies ($\text{SFR}_{\text{Ly}\alpha} \lesssim 2 M_{\odot} \text{ yr}^{-1}$) are main sources of intergalactic CIV absorbers, and such small galaxies play a major role in the metal enrichment of the intergalactic medium at $z \gtrsim 5$.

1. INTRODUCTION

The detection of metal absorption systems at $z > 6$ indicates that the intergalactic medium (IGM) has already been enriched by the end of reionization (e.g., Becker et al. 2006, 2012; Keating et al. 2014). A key question is to understand what the sources of early metals are and how they got distributed throughout the IGM in the post-reionization universe. Theoretical models suggest that galactic superwinds from star-forming galaxies is a main source of the early IGM enrichment. Oppenheimer & Davé (2006) explored high-redshift IGM absorbers in cosmological simulations, employing various prescriptions for galactic outflows to enrich the IGM at $z = 2 - 6$. Oppenheimer et al. (2009) and Finlator et al. (2015) studied the relation between galaxies and CIV absorbers in simulations, and predicted that strong absorbers are the result of outflows from galaxies with stellar masses $M = 10^{7-9} M_{\odot}$, and star formation rates (SFRs) of a few $M_{\odot} \text{ yr}^{-1}$. The separation between the CIV absorber and the associated galaxy is tens of kpc ($\approx 5 - 50$ kpc) from the quasar line of sight. Note the virial radius of such small galaxies is $\approx 7 - 8$ kpc at $z \approx 5 - 6$ (e.g., Wechsler et al. 2002).

At $z > 5$, observations of IGM - galaxy interactions are difficult. In the field of the strong CIV absorber J1030+0524 at $z = 5.7$, Díaz et al. (2011) reached a minimum UV-based star formation of $\sim 5 M_{\odot} \text{ yr}^{-1}$ with deep VLT observations. They identified a galaxy asso-

ciated with CIV absorber at an impact parameter of 79 kpc. Díaz et al. (2014, 2015) further present the large-scale overdensity of Ly α emitters (LAEs) at $z \approx 5.7$ associated with this CIV absorption systems. This survey reached a Ly α -based star formation rate ($\text{SFR}_{\text{Ly}\alpha}$) of $5 M_{\odot} \text{ yr}^{-1}$ and the closest CIV-galaxy pair had an impact parameter of 300 ($213 h^{-1}$) kpc. Nevertheless, these great efforts have not ruled out the possibility that fainter galaxies with small impact parameters may be the source of CIV absorption. To better test theoretical simulations, we need to probe galaxies down to stellar masses of $M \lesssim 10^9 M_{\odot}$ and SFRs of $\approx 1 - 2 M_{\odot} \text{ yr}^{-1}$.

Using HST/ACS narrowband ramp filters, we carried out deep narrow-band imaging of four IGM CIV absorbers at $z = 5 - 6$. We adjusted the ACS ramp filters to the desired wavelength for Ly α detection to search for LAEs in the vicinity of CIV absorbers. The ACS ramp filter has a monochromatic patch of $40'' \times 20''$, corresponding to an area of $250 \text{ kpc} \times 125 \text{ kpc}$ (physical). With the ACS ramp filters, we are able to reach 3σ $\text{SFR}_{\text{Ly}\alpha}$ of $= 1 - 2 M_{\odot} \text{ yr}^{-1}$. Typical (M^*) Lyman break galaxies (LBGs) at $z \approx 5 - 6$ have SFRs of $\sim 7 M_{\odot} \text{ yr}^{-1}$. The depth probed in these observations is much lower than the typical LBGs and previous ground-based observations. This depth also allows us to test the theoretical models of galactic outflows (e.g., Oppenheimer et al. 2009) which predict that the CIV sources have SFRs of $\lesssim 1 M_{\odot} \text{ yr}^{-1}$. In §2, we introduce the HST observations. In §3, we discuss our observational results and the target selection of galaxy candidates. In §4, we discuss

¹ Email: zcai@ucolick.org

the implication of the observations. We convert redshifts to physical distances assuming a Λ CDM cosmology with $\Omega_m = 0.3$, $\Omega_\Lambda = 0.7$ and $h = 0.70$ (h_{70}). Throughout this paper, we use physical distances and AB magnitude.

2. HUBBLE SPACE TELESCOPE OBSERVATIONS

2.1. Sample Selection

The CIV absorbers at $z = 5 - 6$ were selected from the sample of Simcoe et al. (2011). From this sample, we select four secure, strong CIV absorbers at $z = 4.87 - 5.74$ in two QSO sight lines: SDSSJ1030+0524 ($z_{\text{QSO}} = 6.30$) and SDSSJ1306+0356 ($z_{\text{QSO}} = 6.00$). The CIV column densities range from 13.8 cm^{-2} to 14.8 cm^{-2} . These two QSO fields have broadband (F775W, F850LP) images available from Stiavelli et al. (2005). The sample is summarized in Table 1.

2.2. Observations

We devoted 15 orbits to observe four CIV absorber fields in different filters (HST-GO-12860). We used five orbits using FR853N ramp filter for the $z = 5.7$ system, four orbits using F782N for the $z = 5.5$ absorber, and three orbits using F716N for each of the two $z = 4.9$ systems. For each ramp filter, the central wavelength is tuned to the CIV absorption to search for the Ly α emission associated with CIV absorption. The ramp filter has a peak efficiency (70%) spanning 3000 km s^{-1} , much larger than the systematic velocity offset of Ly α to CIV absorber (450 km s^{-1} , Steidel et al. 2010). Our HST observations allow us to measure: (1) Ly α -based star formation rate ($\text{SFR}_{\text{Ly}\alpha}$), (2) projected distances between the galaxies and CIV absorbers, and (3) UV-based star formation rates (SFR_{UV}) or their upper limits. The observations probe $\text{SFR}_{\text{Ly}\alpha} = 2 M_\odot \text{ yr}^{-1}$ at the $4\text{-}\sigma$ level, corresponding to a Ly α flux of $2.2 \times 10^{42} \text{ erg s}^{-1}$ (Kennicutt 1998). Data reduction is performed with Multidrizzle (Koekemoer et al. 2013). Using a uniform $0.6''$ diameter aperture, we calculated the depth of our observations in different bands. The narrowband magnitude for point sources reached the 5σ level of $m_{\text{F716N}} = 26.1$, $m_{\text{F782N}} = 26.0$, and $m_{\text{F853N}} = 26.1$. The broadband observations reached $m_{\text{F850LP}} = 27.8$ and $m_{\text{F775W}} = 27.7$ at the $5\text{-}\sigma$ level. Photometry is performed with SExtractor (Bertin & Arnouts 1996) (Bertin & Arnouts 1996) using the root-mean-square map converted from the inverse variance image generated by Multidrizzle (Casertano et al. 2000).

3. RESULTS

3.1. Selection of Ly α emitter candidates

We select Ly α emitter (LAE) candidates with rest-frame equivalent width (EW) $> 20 \text{ \AA}$. The EW of 20 \AA corresponds to the color selection criteria of $m_{\text{broadband}} - m_{\text{narrowband}} > 0.65$. Also, we require the signal-to-noise ratio (SNR) of the continuum-subtracted flux to be greater than 3. The signal-to-noise is calculated using $m_B - m_{\text{NB}} \geq \Sigma \times \sqrt{\sigma_{\text{NB}}^2 + \sigma_B^2}$, where $\Sigma = 3.0$, and m_{NB} , σ_{NB} , m_B , σ_B representing the magnitudes and errors of the narrowband and broadband. The selection criteria are shown in Fig. 1, Fig. 2, and Fig. 3. Galaxies reside above both red and blue dotted lines are selected. One LAE candidate satisfies the selection criteria in each

of the three CIV absorber fields at $z = 5.74$, $z = 4.95$, and $z = 4.87$. We visually checked individual exposures of these candidates to make sure: (a) their photometry are not affected by cosmic rays; (b) sources do not reside at the detector edges where the photometry is less accurate. We do not detect any LAE candidates associated with the CIV system at $z = 5.52$.

In each figure, we use the following galaxy model to fit the photometry of LAE candidates to derive the flux of Ly α emission, the Ly α -based and UV-based SFR. We use the Bruzual & Charlot (2003) models with a Salpeter Initial Mass Function, a 0.2 solar metallicity ($Z = 0.004$), a continuous star formation history, and an age of 30 Myr (e.g., Ono et al. 2010). We use the Ly α optical depth derived by (Madau 1995) to account for the IGM absorption. Then, we add the dust extinction following Calzetti et al. (2000) with $R_V = A(V)/E(B - V) = 3.1$ for the $z \approx 5.7$ candidates, and set R_V a free parameter for two $z \approx 5.0$ candidates. Further, we added the Ly α emission based on our narrowband observations, assuming the FWHM of Ly α is 300 km s^{-1} (e.g., Jiang et al. 2013).

3.2. Physical Properties of LAE candidates

In Table 1, we provide the physical properties of the three LAE candidates. For the CIV absorber at $z_{\text{abs}} = 5.744$, we detect a LAE candidate with an impact parameter of 42 kpc. This LAE candidate has an expected Ly α luminosity of $L_{\text{Ly}\alpha} = 1.75 \pm 0.44 \times 10^{42} \text{ erg s}^{-1}$, corresponding to the $\text{SFR}_{\text{Ly}\alpha}$ of $2.0 M_\odot \text{ yr}^{-1}$ (e.g., Kennicutt 1998). The SFR_{UV} is estimated to be $4.1 M_\odot \text{ yr}^{-1}$, using the flux density of the best-fit SED around $\lambda_{\text{rest}} = 1500 \text{ \AA}$ (Madau et al. 1998). Diaz et al. (2011) found a LAE at 79 kpc away from the CIV absorber and suggested that this LAE could be the powering source. We do not detect any NB-excess of this source in our deeper HST observations. This source has $m_{\text{F853N}} > 26.30$, $m_{\text{F775W}} = 26.75 \pm 0.09$, $m_{\text{F850LP}} = 26.23 \pm 0.06$, which is inconsistent with a LAE at $z \approx 5.7$.

For the CIV absorber at $z_{\text{abs}} = 4.948$, the impact parameter of the LAE candidate is 163 kpc. The Ly α luminosity is $L_{\text{Ly}\alpha} = 3.27 \pm 0.56 \times 10^{42} \text{ erg s}^{-1}$, corresponding to a $\text{SFR}_{\text{Ly}\alpha} = 3.0 M_\odot \text{ yr}^{-1}$. The SFR_{UV} is $8.7 M_\odot \text{ yr}^{-1}$. For the CIV absorber at $z_{\text{abs}} = 4.866$, there is a LAE candidate with an impact parameter of 205 kpc. The Ly α luminosity is $L_{\text{Ly}\alpha} = 2.72 \pm 0.55 \times 10^{42} \text{ erg s}^{-1}$, corresponding to a $\text{SFR}_{\text{Ly}\alpha} = 2.5 M_\odot \text{ yr}^{-1}$. The UV-based SFR is estimated to be $2.1 M_\odot \text{ yr}^{-1}$. If we further assume a stellar mass (M_*) – SFR relation at $z = 4 - 5$ (e.g., Sparre et al. 2014), the SFR_{UV} -derived stellar mass of these three LAE candidates have stellar masses of $\sim 10^{9.0-9.5} M_\odot$ and halo masses of $\sim 10^{10} M_\odot$.

For the CIV absorber at $z_{\text{abs}} = 5.517$, we do not detect any LAE associated with this absorber, placing a 3σ upper limit on the Ly α luminosity of $1.60 \times 10^{42} \text{ erg s}^{-1}$ and a $3\text{-}\sigma$ upper limit on the $\text{SFR}_{\text{Ly}\alpha} \approx 1.5 M_\odot \text{ yr}^{-1}$.

The main contaminants of high- z LAEs are strong [O II] emitters at lower redshift. For two CIV absorbers at $z \approx 4.9$, we currently have no imaging observations bluer than the Ly α emission. We expect that the contamination rate due to low- z [O II] emission is relatively high. [O II] emitters at $z = 0.91$ ($z = 0.94$) with rest-frame EW $> 61.3 \text{ \AA}$ are contaminants of LAEs at $z = 4.948$

($z = 4.866$) with rest-frame $EW > 20 \text{ \AA}$. From the [O II] luminosity function at $z \approx 1.0$ (Takahashi et al. 2007; Zhu et al. 2009), strong [O II] emitters that can be detected in our depth ($EW > 61.3 \text{ \AA}$, $L_{[\text{OII}]} > 10^{41.0} \text{ erg s}^{-1}$) have a number density of 0.009 Mpc^{-3} , corresponding to ≈ 0.2 per field. For LAE candidates at $z = 5.7$, a number of studies have been conducted at similar redshifts (e.g., Shimasaku et al. 2006; Ouchi et al. 2008, 2017). Spectroscopic confirmations suggest that the contamination rate is $\lesssim 20\%$ at our depth. Future spectroscopic follow-ups must be conducted to confirm or rule out the LAE candidates conclusively.

4. DISCUSSIONS

We find three LAE candidates in the field of three strong CIV absorbers at $z = 5.744$, $z = 4.948$, and $z = 4.866$, respectively. At $z = 5.74$, we detect an impact parameter of 42 physical kpc from the quasar sight line. This is a plausible CIV source which has a $\text{SFR}_{\text{Ly}\alpha}$ of $2 M_{\odot} \text{ yr}^{-1}$ and $\text{SFR}_{\text{UV}} = 4.1 M_{\odot} \text{ yr}^{-1}$. At $z = 4.95$ and $z = 4.87$, we detect two galaxy candidates with impact parameters of 160 kpc and 200 kpc. Here, let us assume galaxies start an outflow at the average redshift when reionization occurs ($z \approx 9$ from Planck Observations, Adam et al. 2016), then at $z \approx 5.7$, the momentum driven winds ($v \approx 200 \text{ km s}^{-1}$) travel about 90 kpc, less than the impact parameter we observed. Also, simulations (e.g., Oppenheimer et al. 2009) predict that impact parameters should be $\lesssim 50$ kpc to yield strong CIV absorption with $N_{\text{CIV}} \gtrsim 10^{14} \text{ cm}^{-2}$. We do not detect LAEs associated with the CIV absorber at $z = 5.52$. We place $3\text{-}\sigma$ upper limits of $\text{SFR}_{\text{Ly}\alpha} \approx 1.5 M_{\odot} \text{ yr}^{-1}$ in each of the three non-detection fields.

4.1. Probing CIV enrichment using LAEs

One potential issue is that not all star forming galaxies have Ly α emission that can be selected using the LAE selection technique. Schenker et al. (2012) showed that 60% galaxies with absolute magnitude of $-20.3 < M_{\text{UV}} < -18.7$ have Ly α EW greater than 20 \AA . Our observations probe galaxies down to $M_{\text{UV}} \approx -18.5$ in $3\text{-}\sigma$, indicating a high completeness of using LAE technique to select galaxies in our survey. Another issue is whether LAE candidates we detected are physically associated with the CIV absorbers. Observationally, we can evaluate this issue by calculating the number of galaxies expected in random fields: if $\ll 1$ galaxies is expected within an impact parameter in random fields, then galaxies detected within these impact parameters are more likely to be sources of CIV systems (e.g., Díaz et al. 2014). This is because CIV absorbers are expected to be clustered with the physically-associated galaxies. The LAE candidate we detected at $z = 5.74 \pm 0.07$ is the first source reported at $z > 5$ to be projected ≈ 40 kpc away from a CIV absorber. From the luminosity function at $z = 5.7$ (Ouchi et al. 2008; Konno et al. 2017), the $L_{\text{Ly}\alpha}^* = 6.8 \times 10^{42} \text{ erg s}^{-1}$ and $\phi^* = 7.7 \times 10^{-4} \text{ Mpc}^{-3}$. Our limiting Ly α luminosity is $0.26 \times L_{\text{Ly}\alpha}^*$. The width of the FR853N ramp filter corresponds to a redshift interval of $\Delta z = 0.14$. The expected number of finding a LAE in random fields with $L_{\text{Ly}\alpha} \geq 0.26 \times L_{\text{Ly}\alpha}^*$ and at impact parameters of ≤ 42 kpc is 0.01. The number of

faint galaxies with $L = 0.01 - 0.26 \times L_{\text{Ly}\alpha}^*$ (below our detection limit) and an impact parameter within 42 kpc is 0.2. Thus, there is a relatively small probability to find such a LAE in random fields. If this LAE candidate is confirmed by future deep spectroscopy, then one can conclude that this galaxy is highly likely to be the source of the CIV absorber at $z = 5.744$.

For two CIV absorbers at $z \approx 5$, the expected number of LAEs with $L_{\text{Ly}\alpha} \geq 0.26 \times L_{\text{Ly}\alpha}^*$ and an impact parameter of ≈ 200 kpc is 0.5. The number of faint LAEs ($L_{\text{Ly}\alpha} = 0.01 - 0.26 \times L_{\text{Ly}\alpha}^*$) is expected to be ≈ 10 in random fields. As a result, it is unlikely that the LAE candidates we detected at $z \approx 5.0$ are sources of the CIV absorbers, and thus we treat these two sight lines as non-detections.

4.2. Constraining IGM enrichment models

From our one detection and three non-detections, we conclude that strong CIV systems at $z \approx 5 - 6$ do not generally lie close to galaxies identified as LAEs with $\text{SFR} \gtrsim 2 M_{\odot} \text{ yr}^{-1}$. This is surprising because strongly star-forming galaxies are expected to be driving the strongest outflows at these epochs, enriching the early IGM. Models generically predict early, widespread enrichment of metals (e.g. Madau et al. 2001; Oppenheimer & Davé 2008), such that $z \gtrsim 5$ represents the first epoch of IGM enrichment. Given this, the most straightforward interpretation of our result is that early enrichment is dominated, at least in a volumetric sense, by small galaxies with $\text{SFR} \lesssim 2 M_{\odot} \text{ yr}^{-1}$.

There are two important caveats to this result. First, our observations cannot select LBGs without strong Ly α emission. However, as noted in the previous section, LBGs and LAEs are often coincident at these epochs (60% of LBGs at $z = 5 - 6$ are LAEs) (e.g., Schenker et al. 2012). If the 40% that are not LAEs are randomly associated with LBGs, then the probability of all four CIV systems being undetected is $0.4^4 (< 3\%)$. Second, our selection disfavors the detection of massive dust-obscured galaxies. Such galaxies are metal-rich and have high SFR, so potentially we could be missing these sources. However, typical high-SFR objects at these epochs should not be heavily dust-obscured (e.g. Ono et al. 2010; Finkelstein et al. 2012). Future sub-millimeter observations would be required to rule out this explanation conclusively.

Setting aside the caveats, our conclusion represents an important constraint on models of early metal production and dissemination. Such models began by post-processing metal distributions onto cosmological simulations (e.g. Davé et al. 1998; Aguirre et al. 2001), but the introduction of outflows into simulations by Springel & Hernquist (2003) enabled self-consistent IGM enrichment. Oppenheimer & Davé (2006) showed that a momentum-driven outflow model in which small galaxies have higher mass loading (i.e. outflow rate relative to SFR) yielded better agreement with CIV enrichment at $z \sim 2 - 4$, as compared to models where the mass loading is independent of galaxy mass. Oppenheimer et al. (2009) extended these results to $z \sim 6$, and showed that the high mass loading factors in small galaxies resulted in early enrichment in accord with CIV data, despite a fairly small metal volume filling factor of a couple

percent. They further predicted that strong absorbers ($N_{\text{CIV}} = 10^{13.8-14.8} \text{ cm}^{-2}$) arise from outflows from galaxies with stellar masses $\sim 10^{7-9} M_{\odot}$ and impact parameters from a few kpc up to 50 kpc. These predictions are consistent with our observational results.

Using cosmological simulations, Finlator et al. (2013) introduced on-the-fly radiative transfer into cosmological simulations and examined early metal enrichment in conjunction with an inhomogeneous ionising background to determine the impact of local UVB fluctuations on the ionisation state. They argued that the mass scale of halos hosting OI absorbers was $10-100\times$ smaller than typical LBGs at $z \sim 6$, which is consistent with our results if OI and C IV absorption arise around similar systems. In contrast, Keating et al. (2016) examined early IGM enrichment in the Sherwood and Illustris simulations, and found that galaxies associated with strong ($\text{EW} > 1 \text{ \AA}$) CIV absorbers have halo masses of $M > 10^{11} M_{\odot}$, and impact parameters of 10-30 kpc. These results seem to be less in agreement with our results at face value, although a more careful comparison is warranted. This is interesting because Illustris utilizes a mass loading factor that increase to lower masses even more rapidly than in momentum-driven wind models. Hence other factors such as local density and ionisation may be playing a key role. It could be that the Keating et al. (2016) and Nelson et al. (2015) models are predicting strong CIV from dust-obscured galaxies that would be missed

by our LBG/LAE survey.

To summarize, we present the detection of one plausible CIV source at $z = 5.7$ with a projected distance of 42 kpc and a $\text{SFR}_{\text{Ly}\alpha} = 1.75 \pm 0.44 M_{\odot} \text{ yr}^{-1}$. Also, we found two LAE candidates in the field of two CIV absorbers at $z = 4.95$ and $z = 4.87$ with projected distances of 163 and 205 kpc, respectively. But the impact parameters are much larger than that predicted by simulations, making them unlikely to be CIV sources. We do not detect CIV-associated LAEs at $z = 5.52$. From our observations, no CIV-associated LAEs have impact parameters $\lesssim 40$ kpc with $\text{SFR}_{\text{Ly}\alpha} \geq 1.5 M_{\odot} \text{ yr}^{-1}$ (3σ limit). Particularly, for strongest absorbers with $\text{EW} > 2 \text{ \AA}$, we do not detect LAEs with $3\sigma \text{ SFR}_{\text{Ly}\alpha} \geq 1.4 M_{\odot} \text{ yr}^{-1}$. Our observations provide strong constraints on models of early enrichment in simulations. Future facilities, including James Webb Space Telescope (*JWST*), will probe IGM-galaxy relation down to a much fainter galaxy population where some models predict that the CIV arises.

Acknowledgement: We thank the referee for valuable comments. ZC thanks Marcel Neeleman for his useful comments. ZC, XF thank the support from the US NSF grant AST 11-07682. Support for part of this work was also provided by NASA through the Hubble Fellowship grant HST-HF2-51370 awarded by the Space Telescope Science Institute, which is operated by the Association of Universities for Research in Astronomy, Inc., for NASA, under contract NAS 5-26555.

REFERENCES

- Aguirre, A., Hernquist, L., Schaye, J., et al. 2001, *ApJ*, 561, 521
 Alvarez, M. A., Finlator, K., & Trenti, M. 2012, *ApJ*, 759, L38
 Becker, G. D., Sargent, W. L. W., Rauch, M., & Simcoe, R. A. 2006, *ApJ*, 640, 69
 Becker, G. D., Sargent, W. L. W., Rauch, M., & Carswell, R. F. 2012, *ApJ*, 744, 91
 Bertin, E., & Arnouts, S. 1996, *A&AS*, 117, 393
 Bruzual, G., & Charlot, S. 2003, *MNRAS*, 344, 1000
 Calzetti, D., Armus, L., Bohlin, R. C., et al. 2000, *ApJ*, 533, 682
 Casertano, S., de Mello, D., Dickinson, M., et al. 2000, *AJ*, 120, 2747
 Cooksey, K. L., Prochaska, J. X., Chen, H.-W., Mulchaey, J. S., & Weiner, B. J. 2008, *ApJ*, 676, 262-285
 Cooksey, K. L., Kao, M. M., Simcoe, R. A., O’Meara, J. M., & Prochaska, J. X. 2013, *ApJ*, 763, 37
 Davé, R., Hellsten, U., Hernquist, L., Katz, N., & Weinberg, D. H. 1998, *ApJ*, 509, 661
 Davé, R., Finlator, K., & Oppenheimer, B. D. 2006, *MNRAS*, 370, 273
 Díaz, C. G., Ryan-Weber, E. V., Cooke, J., Pettini, M., & Madau, P. 2011, *MNRAS*, 418, 820
 Díaz, C. G., Ryan-Weber, E. V., Cooke, J., Koyama, Y., & Ouchi, M. 2015, *MNRAS*, 448, 1240
 Díaz, C. G., Koyama, Y., Ryan-Weber, E. V., et al. 2014, *MNRAS*, 442, 946
 D’Odorico, V., Calura, F., Cristiani, S., & Viel, M. 2010, *MNRAS*, 401, 2715
 D’Odorico, V., Cupani, G., Cristiani, S., et al. 2013, *MNRAS*, 435, 1198
 Finlator, K., Muñoz, J. A., Oppenheimer, B. D., et al. 2013, *MNRAS*, 436, 1818
 Finlator, K., Thompson, R., Huang, S., et al. 2015, *MNRAS*, 447, 2526
 Finkelstein, S. L., Papovich, C., Salmon, B., et al. 2012, *ApJ*, 756, 164
 Finkelstein, S. L., Ryan, R. E., Jr., Papovich, C., et al. 2015, *ApJ*, 810, 71
 Jiang, L., Egami, E., Mechtley, M., et al. 2013, *ApJ*, 772, 99
 Keating, L. C., Haehnelt, M. G., Becker, G. D., & Bolton, J. S. 2014, *MNRAS*, 438, 1820
 Keating, L. C., Puchwein, E., Haehnelt, M. G., Bird, S., & Bolton, J. S. 2016, *MNRAS*, 461, 606
 Kennicutt, R. C., Jr. 1998, *ARA&A*, 36, 189
 Koekemoer, A. M., Ellis, R. S., McLure, R. J., et al. 2013, *ApJS*, 209, 3
 Konno, A., Ouchi, M., Shibuya, T., et al. 2017, arXiv:1705.01222
 Madau, P. 1995, *ApJ*, 441, 18
 Madau, P., Pozzetti, L., & Dickinson, M. 1998, *ApJ*, 498, 106
 Madau, P., Ferrara, A., & Rees, M. J. 2001, *ApJ*, 555, 92
 Nelson, D., Pillepich, A., Genel, S., et al. 2015, *Astronomy and Computing*, 13, 12
 Ono, Y., Ouchi, M., Shimasaku, K., et al. 2010, *ApJ*, 724, 1524
 Oppenheimer, B. D., & Davé, R. 2006, *MNRAS*, 373, 1265
 Oppenheimer, B. D., & Davé, R. 2008, *MNRAS*, 387, 577
 Oppenheimer, B. D., Davé, R., & Finlator, K. 2009, *MNRAS*, 396, 729
 Ouchi, M., Shimasaku, K., Akiyama, M., et al. 2008, *ApJS*, 176, 301-330
 Ouchi, M., Harikane, Y., Shibuya, T., et al. 2017, arXiv:1704.07455
 Ryan-Weber, E. V., Pettini, M., & Madau, P. 2006, *MNRAS*, 371, L78
 Ryan-Weber, E. V., Pettini, M., Madau, P., & Zych, B. J. 2009, *MNRAS*, 395, 1476
 Schenker, M. A., Stark, D. P., Ellis, R. S., et al. 2012, *ApJ*, 744, 179
 Simcoe, R. A., Cooksey, K. L., Matejek, M., et al. 2011, *ApJ*, 743, 21
 Sparre, M., Hartoog, O. E., Krühler, T., et al. 2014, *ApJ*, 785, 150
 Stark, D. P. 2016, *ARA&A*, 54, 761
 Stiavelli, M., Djorgovski, S. G., Pavlovsky, C., et al. 2005, *ApJ*, 622, L1
 Shimasaku, K., Kashikawa, N., Doi, M., et al. 2006, *PASJ*, 58, 313
 Springel, V., & Hernquist, L. 2003, *MNRAS*, 339, 289
 Songaila, A. 2001, *ApJ*, 561, L153
 Takahashi, M. I., Shioya, Y., Taniguchi, Y., et al. 2007, *ApJS*, 172, 456

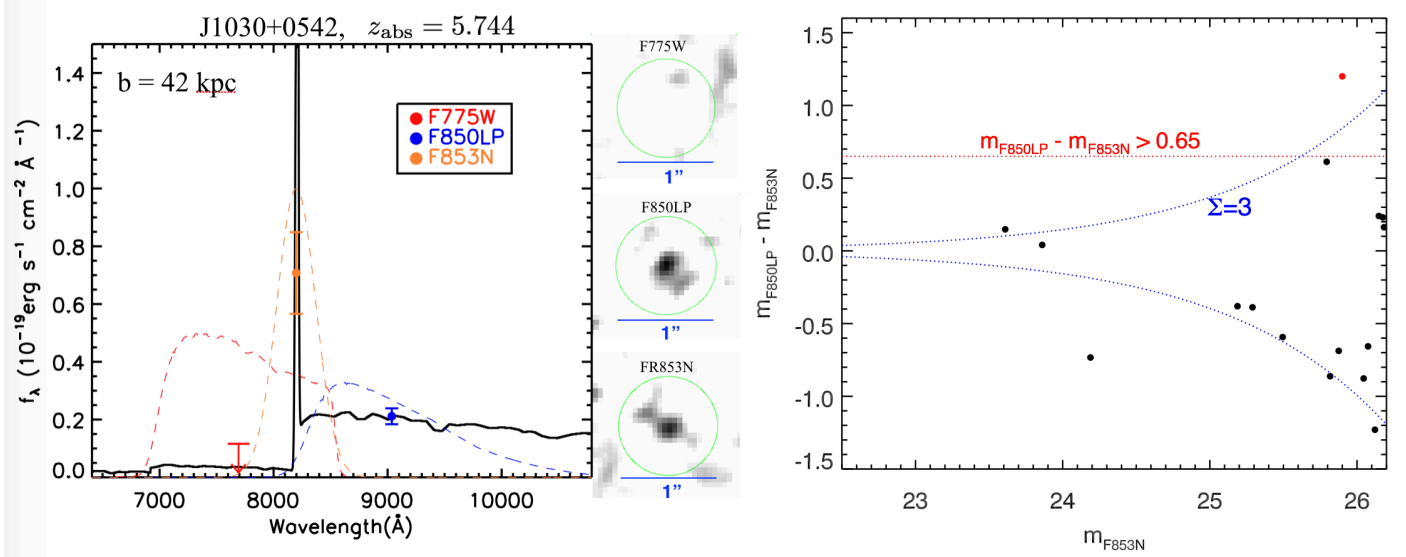


FIG. 1.— The left panel shows the best-fit spectrum (black line) of the candidate of the Ly α emitter (LAE) associated with the CIV absorber at $z = 5.744$. The impact parameter between this LAE candidate and the CIV absorber is 42 kpc. The filter response curves of F775W (red dashed line), F850LP (blue dashed line) and ACS ramp filter (yellow dashed line) are overplotted. In addition, the photometry in three different bands are overplotted at the effective wavelength of each filter. The right panel shows the color - magnitude diagram of galaxies within the monochromatic field of view of FR853N field. The color selection criteria for the LAE candidates (red dot) are broadband (B) - narrowband (NB) $> 0,65$ (red horizontal dotted line) and $m_B - m_{NB} \geq \Sigma \times \sqrt{\sigma_{NB}^2 + \sigma_B^2}$, where $\Sigma = 3.0$ (blue dotted line).

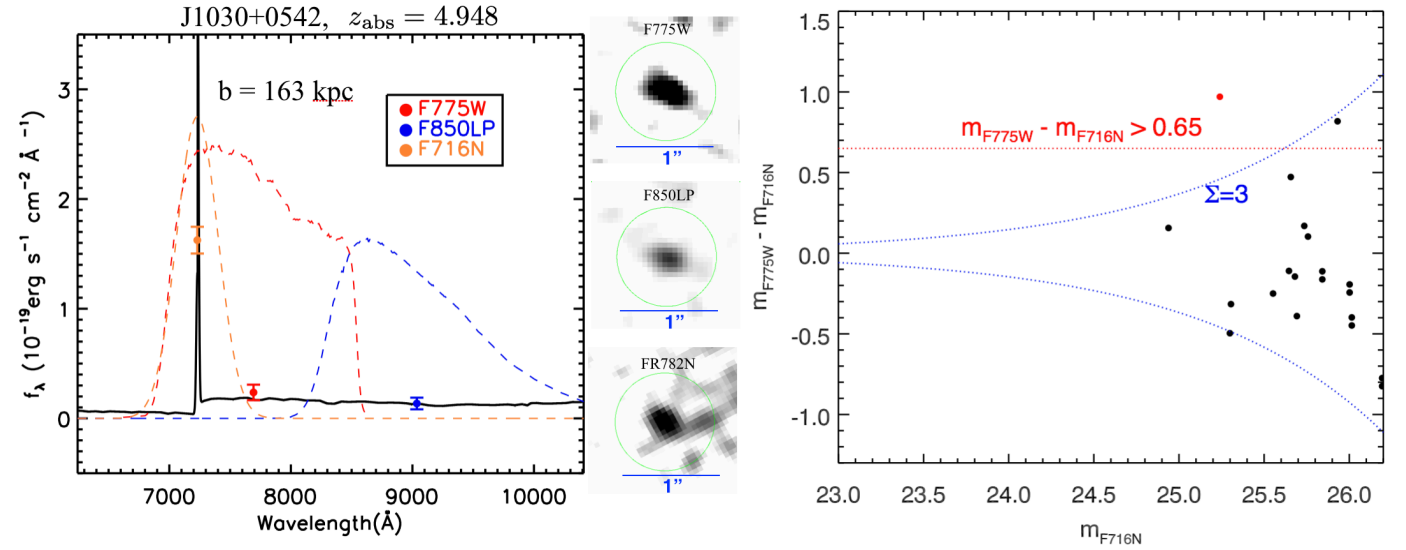


FIG. 2.— Same format as the Figure 1, presenting the photometry and the selection of LAE candidates in the CIV absorber field at $z = 4.948$.

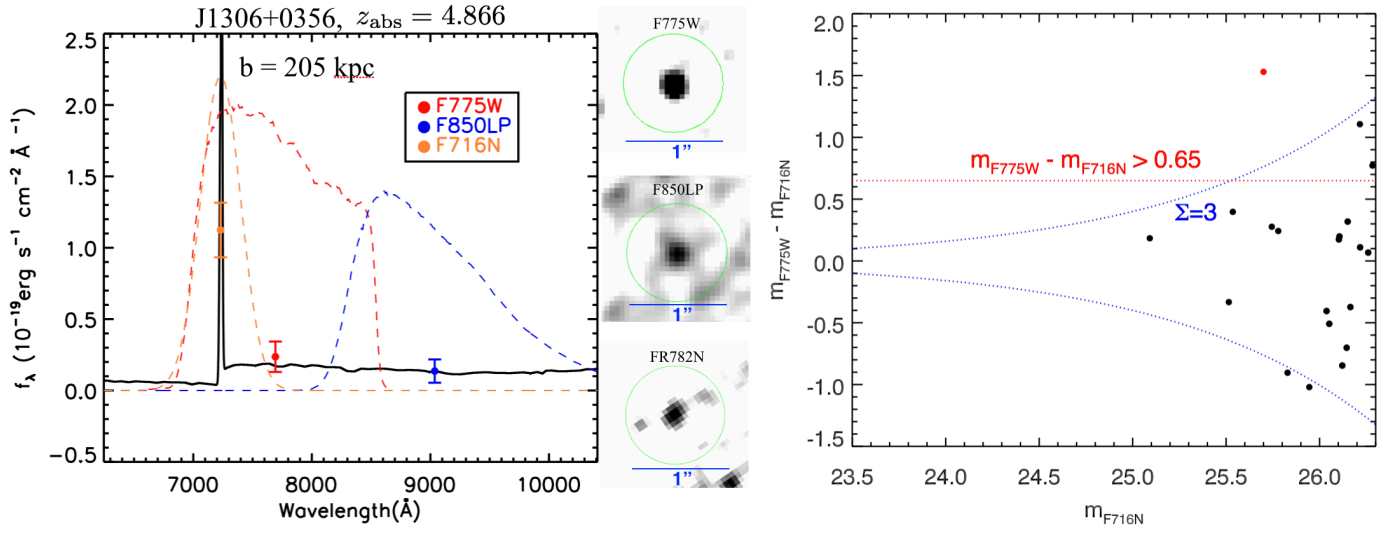


FIG. 3.— Same format as the Figure 1, showing the photometry and the selection of LAE candidates in the CIV absorber field at $z = 4.866$.

TABLE 1
SUMMARY OF THE CIV-ASSOCIATED Ly α EMITTER CANDIDATES

RA	DEC	z_{CIV}	$\text{Log}[\frac{N_{\text{CIV}}}{\text{cm}^2}]$	EW _{CIV} (\AA)	Filter	NB	F775W	F850LP	$L_{\text{Ly}\alpha}$ ($10^{42} \text{ erg s}^{-1}$)	SFR _{Lyα} ($M_{\odot} \text{ yr}^{-1}$)	SFR _{UV} ($M_{\odot} \text{ yr}^{-1}$)	b (kpc)	EW _{Lyα} (\AA)
10:30:26.746	+5:24:59.76	5.744	14.00 ± 0.04	1.3	FR853	25.90 ± 0.21	$2\sigma > 28.0$	27.10 ± 0.13	1.75 ± 0.44	2.0	4.1	42	44 \AA
		5.517	14.02 ± 0.04	0.6	FR782	$2\sigma \geq 26.8$	$2\sigma \geq 27.9$	$2\sigma \geq 28.0$	$3\sigma \leq 1.3$	$3\sigma \leq 1.2$	$3\sigma \leq 1.5$	≥ 125	
10:30:27.486	+05:25:20.15	4.948	13.76 ± 0.11	0.5	FR716	25.24 ± 0.12	26.21 ± 0.06	26.04 ± 0.06	3.27 ± 0.56	3.0	8.7	163	28 \AA
13:06:06.161	+03:56:32.94	4.866	14.80 ± 0.01	2.6	FR716	25.70 ± 0.17	27.23 ± 0.12	27.56 ± 0.19	2.72 ± 0.55	2.5	2.1	205	76 \AA